Electronic fingerprints for diverse interactions of methanol with various Zn-based systems

Shweta Mehta and Kavita Joshi*

Physical and Materials Chemistry Division,

CSIR-National Chemical Laboratory,

Dr. Homi Bhabha Road, Pashan, Pune 411008, India and

Academy of Scientific and Innovative Research (AcSIR), Sector 19,

Kamla Nehru Nagar, Ghaziabad, Uttar Pradesh- 201002, India.

(Dated: December 29, 2022)

Abstract

We have investigated various Zn-based catalysts for their interaction with methanol (MeOH). MeOH is one of the most critical molecules being studied extensively, and Zn-based catalysts are widely used in many industrially relevant reactions involving MeOH. We note that the same element (Zn and O, in the present study) exhibits different catalytic activity in different environments. The changing environment is captured in the underlying electronic structure of the catalysts. In the present work, we compared the electronic structure of Zn-based systems, i.e., $ZnAl_2O_4$ and ZnO along with oxygen preadsorbed Zn (O-Zn) and metallic Zn. We demonstrate the one-to-one correlation between the pDOS of the bare facet and the outcome of that facet's interaction (i.e. either adsorption or dissociation of MeOH) with MeOH. These findings would pave the way towards the in-silico design of catalysts.

* k.joshi@ncl.res.in

I. INTRODUCTION

For conversion of methanol to any value added product dissociation of its O-H and/or C-H bond is the primary step. Considering the importance of MeOH in the chemical industry as feedstock or fuel, its interaction with various catalysts is studied extensively. The interaction of methanol with metal surfaces like Al[1], Si[2], Ge[3], Fe[4], Ru[5], Rh[6], Ni[7], Pd[8], Pt[9], Cu[10], Ag[11], Au[12] has been extensively investigated using both experimental and theoretical methods. The activation barrier for inert metals such as Au and Ag is very high, almost of the order of 1.5 eV, while for Pd and Pt, it reduces to $\approx$ 0.80 eV. However one would like to replace precious metals by other earth abundant metals for the economical viability. This encourages further investigations into non-precious metals for methanol dissociation. Cu surfaces have also been studied in detail for MeOH interaction.[10, 13, 14] The activation barrier for O-H bond dissociation of MeOH on Cu surfaces is as low as 0.38 eV. In a recent experimental study, Roey et al. demonstrated the methanol decomposition on various Cu surfaces such as (100), (110), and (111) at ambient conditions.[15] They observed that methanol readily decomposes to methoxy on all these surfaces at atmospheric pressure and room temperature. They also report that the kinetics of conversion of methanol to carbon monoxide is structure sensitive and depends on the surface environment. Adsorption of oxygen on metal surfaces affects their reactivity by altering geometric and electronic properties.[16–19] Oxygen binds strongly with almost all metals and triggers surface reconstruction. This reconstruction either facilitates adsorption or blocks the active sites of catalyst. Also, the higher electronegativity of oxygen as compared to metals leads to redistribution of charge density on metal surfaces and hence affect their chemical reactivity.[20] Methanol decomposition has also been investigated in the presence of preadsorbed oxygen atoms on various metal surfaces.[21–24] Xu et al. investigated the interaction of methanol on oxygen-preadsorbed Au(111) surface by employing DFT.[23] They report that the

activation barrier for dissociation of the O-H bond of methanol reduces to 0.41 eV, which is one-fourth of the barrier for bare Au(111) surface (1.58 eV). Similarly, Aljama et al. demonstrated the conversion of methanol to formaldehyde at Ag(111) surface using DFT and microkinetic modeling.[24] They observed that preadsorbed oxygen enhances the reactivity of the Ag surface by reducing the activation barrier to 0.81 eV, which is significantly lower than the clean surface (2.85 eV). This manifests effect of preadsorbed oxygen on metal surfaces in enhancing the MeOH decomposition. To our knowledge, no studies report the interaction of methanol with zinc surfaces. In the present work, we have examined the interaction of MeOH on various Zn surfaces viz. $(10\bar{1}0)$, $(10\bar{1}1)$, and $(10\bar{1}3)$ to demonstrate the structure-activity relationship. Effect of oxygen adsorption on the interaction of MeOH with Zn surfaces has also been explored in detail. The activation barrier of O-H bond dissociation significantly reduces on preadsorbed oxygen compared to the pure metallic surface.

On the other hand, it is very well established that the metal oxides exhibit higher catalytic activity than pure metallic surfaces due to presence of various acidic and basic sites. Various metal oxides like MgO,[25] Al_2O_3,[26] Ga_2O_3,[27] TiO_2,[28] CeO_2,[29] and ZnO[30] have been extensively investigated for their interaction with methanol. It is common to all metal oxides, that, anionic oxygen atoms favor the dehydrogenation of MeOH by forming hydroxide with H_{MeOH}, while the dissociated fragments are stabilized over cationic metal atoms. Spontaneous dissociation of methanol is reported by Liu et al. on low index CeO2 surfaces.[29] They investigated the interaction of methanol with (100), (110), and (111) facets of CeO_2 by employing DFT. They report that the interaction of methanol with the facet is highly dependent on the arrangement of atoms on the facet. Spontaneous dissociation of O-H bond of methanol takes place on the (100) and (110) facet while only molecular adsorption at (111) facet. In our previous study, we have also discussed in detail the interaction of methanol with ZnO [31, 32] We elaborate on the site-dependent interaction of methanol (molecular adsorption or dissociation) on various ZnO surfaces. Further,

we have also investigated interaction of MeOH with $ZnAl_2O_4$.[33] Our periodic DFT calculations demonstrated that the dissociation of methanol is thermodynamically favorable outcome at the $ZnAl_2O_4$ facets.

Our previous work demonstrated that the composition as well as facets play a crucial role in determining the outcome of the interaction. First, we investigated interaction of MeOH with a mixed metal oxide like $ZnAl_2O_4$ followed by metal oxide like ZnO. In the present work, we investigate the interaction of methanol with various Zn metal surfaces as well as oxygen adsorbed Zn facets by exploiting periodic DFT. Thus, we are reducing the complexity to understand factors associated with a particular outcome. In these series of virtual experiments the outcomes are either adsorption of MeOH (physisorption or chemisorption) or spontaneous dissociation of O-H bond. It is indispensable to investigate the underlying electronic structure to understand the rationality behind these interactions. Our group's work over the years shows a clear-cut trend in the interaction of MeOH with Zn-based facets. In this work, we analyze all the surfaces studied so far to determine the correlation between the electronic structure of bare facets and the outcome of MeOH adsorption. The ultimate goal of any DFT based computation is to understand the results in terms of underlying electronic structure, derive trends, and gain predictive power. This work is an attempt in that direction.

II. COMPUTATIONAL DETAILS:

All the calculations are carried out within the Kohn-Sham formalism of DFT. Projector Augmented Wave potential[34] is used, with Perdew Burke Ernzerhof (PBE) approximation for the exchange-correlation and generalized gradient approximation,[35] as implemented in planewave, pseudopotential based code, Vienna Ab initio Simulation Package (*VASP*).[36] The bulk unit cell is taken from the materials project.[37] The bulk lattice parameters upon optimization are a = 2.62 Å and c = 5.02 Å which

are in agreement with the experimentally measured (a = 2.66 Å, c = 4.95 Å).[38] Two flat facets ($10\bar{1}0$) and ($10\bar{1}1$) of Zn are modeled as slab by cleaving a surface with 3x3 periodicity in x and y direction with 4 layers using Quantumwise-VNL-2017.1.[39] The step facet ($10\bar{1}3$) is cleaved using 4x1 periodicity in x and y direction with 4 layers. Bottom layer is fixed and rest all layers and adsorbate are fully relaxed for all surface calculations. Van der Waals corrections are applied to account dynamic correlations between fluctuating charge distribution by employing Grimme method (DFT-D2).[40] It is observed that 20 Å of vacuum is sufficient to avoid interaction between adjacent images of planes along the z-direction. Geometry optimization is carried out with a force cutoff of 0.01 eV/Å on the unfixed atoms and the total energies are converged below 10^{-4} eV for each SCF cycle. A Monkhorst-Pack grid of 3x2x1, 4x2x1, and 2x2x1 is used for ($10\bar{1}0$), ($10\bar{1}1$), and ($10\bar{1}3$) slabs respectively. The difference in energies is less than 4 meV/atom upon using finer mesh. Entire surface is scanned by placing the MeOH molecule at various available unique sites. To compare the interaction of methanol at these sites, interaction energy is calculated using the formula: $E_{MeOH/Zn} = E_{MeOH+Zn}$ - (E_{Zn} + E_{MeOH}) where $E_{MeOH+Zn}$ is energy of the system when MeOH is placed on the Zn surface, E_{Zn} is energy of the bare surface and E_{MeOH} is energy of the MeOH molecule. Further to investigate the effect of oxygen adsorption on reactivity of Zn surfaces, we placed an oxygen atom on all the facets. The interaction energy for oxygen adsorption is calculated using following formula: $E_{O/Zn} = E_{O+Zn}$ - (E_{Zn} + 1/2 E_{O2}) where E_{O+Zn} is energy of the system when oxygen atom is placed on the surface, E_{Zn} is energy of the bare surface and E_{O2} is energy of the isolated O_2 molecule. Also, the interaction energy of methanol adsorption on oxygen preadsorbed Zn surface is calculated using formula: $E_{MeOH/O-Zn}$ = $E_{MeOH+O-Zn}$ - (E_{O+Zn} + E_{MeOH}) Here, $E_{MeOH+O-Zn}$ is the energy of system with methanol adsorbed on oxygen preadsorbed Zn surface. To understand the site specific adsorption pattern, the site-dependent projected Density of States (pDOS) are calculated with denser k-mesh using LOBSTER.[41] The activation barrier for O-

H bond dissociation of methanol is computed using the climbing image-nudged elastic band (CI-NEB) method for both clean and oxygen preadsorbed surfaces.[42] Three images are considered for transition state calculations using a force convergence of 0.1 eV/Å. The computational details of ZnO and $ZnAl_2O_4$ are discussed in detail in our previous papers.[31–33]

III. RESULTS AND DISCUSSION

The rational design of a catalyst for any reaction requires consideration of several parameters like material abundance, cost, the reactivity of the catalyst, reaction conditions, selectivity of products, etc. Some factors, like material abundance and cost, are out of our control. However, the catalytic properties could be altered/improved by understanding its functionality at the atomistic level. Zn-based catalysts are extensively used in many reactions[43–46] because of the abundance of Zn (24^{th} in the earth's crust), inexpensiveness, and safe handling methods. In the present work, we investigate the interaction of MeOH with a series of Zn-based catalysts to understand how the environment changes the properties of a catalyst. We will be comparing the interaction of MeOH with various facets of Zn, oxygen-preadsorbed Zn(O-Zn), ZnO, and finally, with $ZnAl_2O_4$ to understand the reactivity of these catalysts at the electronic level.

We begin by discussing the interaction of methanol with different metallic Zn surfaces. We have modelled $(10\bar{1}0)$, $(10\bar{1}1)$, and $(10\bar{1}3)$ facets of Zn because they exhibit the most prominent peaks in the XRD. Top and side views of all these facets are shown in Fig. SI-1. All these facets are scanned by placing methanol at various inequivalent sites. Before detailed discussions, we note that the physisorption and chemisorption of methanol is explained on the basis of O-H bond-length of methanol upon adsorption. Physisorption of MeOH is accompanied by surface reconstruction of the flat facets, whereas the step facet does not show any rearrangement of surface

TABLE I: Interaction energy ($E_{MeOH/Zn}$/$E_{MeOH/O-Zn}$) (eV), O-H bond-length (Å) of MeOH at various inequivalent sites of $(10\bar{1}0)$, $(10\bar{1}1)$, and $(10\bar{1}3)$ facets of pristine zinc (in black color) and oxygen preadsorbed Zn (in blue color). For O-Zn, the O_{surf}-H_{MeOH} bond-length is shown in parenthesis. In all the cases, irrespective of its initial position, MeOH always diffuses on the surface and adsorb with its oxygen ontop of Zn. However, variation in the relative orientation of MeOH with respect to surface results into observed variation in E_{int}. The thermodynamically most favorable configuration at each facet is represented by numbers in bold.

Initial positions	$(10\bar{1}0)$		$(10\bar{1}1)$		$(10\bar{1}3)$	
	$E_{MeOH/Zn}$ / $E_{MeOH/O-Zn}$ (eV)	O-H BL (Å)	$E_{MeOH/Zn}$ / $E_{MeOH/O-Zn}$ (eV)	O-H BL (Å)	$E_{MeOH/Zn}$ / $E_{MeOH/O-Zn}$ (eV)	O-H BL (Å)
Top	-3.37	0.98	-1.31	0.98	**-0.67**	**0.99**
	-1.66	0.98(3.28)	-0.59	0.99(1.87)	**-1.01**	**1.05(1.49)**
Bridge	—	—	-1.26	0.98	—	—
	—	—	-0.63	0.99(1.76)	—	—
SB	**-4.09**	**0.99**	—	—	-0.57	0.98
	-3.26	**0.99(3.48)**	—	—	-0.93	1.05(1.51)
LB	-3.36	0.98	—	—	-0.64	0.99
	-1.57	0.98(6.47)	—	—	-1.01	1.05(1.49)
4FH/3FH	-3.23	0.99	**-1.35**	**0.98**	-0.64	0.99
	-1.98	0.99(3.44)	**-0.72**	**0.99(1.86)**	-0.64	0.99(6.96)
Top_s	—	—	-1.32	0.98	—	—
	—	—	-0.61	0.99(1.87)	—	—

atoms. This rearrangement of surface atoms also reflects in the lowering of interaction energy of MeOH (refer to Tab.I). In Tab.I, we have noted the interaction energy and O-H bond-length of methanol on all three facets of metallic Zn (in black color) and oxygen preadsorbed Zn (in blue color). The bond-length between O_{surf}-H_{MeOH} are

shown in brackets for all facets of O-Zn. In all the cases, irrespective of the initial position, upon optimization, methanol diffuses on the surface and adsorb ontop of Zn. However, in Tab.I, we have noted the initial position where methanol was placed to distinguish each configuration. The thermodynamically most stable configuration for each facet is shown in bold numbers. The interaction energies for $(10\bar{1}0)$ facets are significantly larger because, the reconstruction energies are buried in it. However, to normalize the interaction energy for all systems, we have excluded the reconstruction energy and noted in Tab.II as WOR. The extent of reconstruction is significant for the $(10\bar{1}0)$ facet because of its open structure and is minimal or absent for the other two facets [$(10\bar{1}1)$, $(10\bar{1}3)$]. The reconstruction on $(10\bar{1}0)$ causes the rearrangement of atoms on the surface, which resembles that of the $(10\bar{1}1)$ facet.

As discussed earlier, exposing a metal surface to oxygen alters its reactivity considerably. To understand the effect of oxygen adsorption on the reactivity of zinc facets, we have adsorbed atomic oxygen on all these facets, as shown in Fig. SI-2. The oxygen on the $(10\bar{1}0)$ surface diffuses to the subsurface layer, while on the other two facets [$(10\bar{1}1)$ and $(10\bar{1}3)$], it adsorbs on the surface. Closed packing of atoms on the $(10\bar{1}1)$ and $(10\bar{1}3)$ facets doesn't favor oxygen diffusion in the subsurface layer.

We placed MeOH at various unique sites of oxygen-preadsorbed Zn surfaces. For pristine metallic surfaces, the MeOH physisorbed on the surface with no elongation in the O-H bond. Oxygen adsorption causes activation of the methanol on the step facet of O-Zn. Representative cases of MeOH adsorption on Zn and oxygen-preadsorbed Zn are shown in Fig.1 (the upper panel and lower panel represent MeOH adsorption at pristine Zn and oxygen-preadsorbed Zn surfaces, respectively). The $(10\bar{1}0)$ facet of Zn undergoes substantial reconstruction upon adsorption of methanol as evident from upper panel of Fig.1-(a).

Although preadsorbed oxygen enhances the catalytic activity of metal surfaces, the reactivity depends on several other factors, such as the structural arrangement of atoms, coordination numbers, and effective charge on surface atoms. As evident from

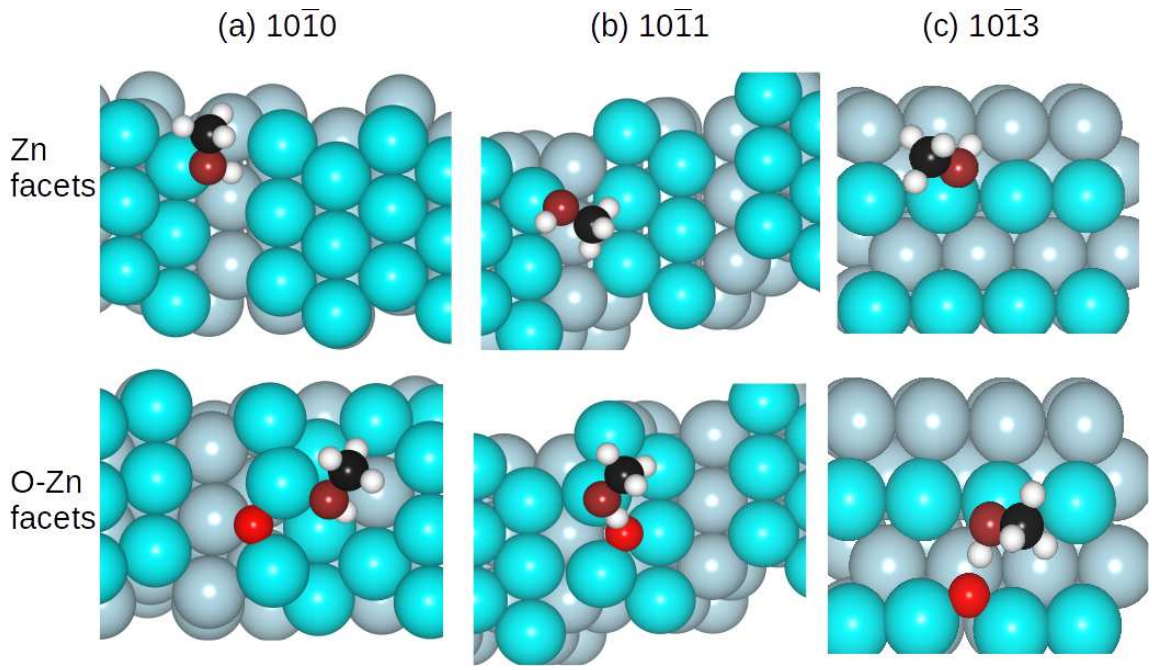

FIG. 1: Interaction of methanol with various facets of pristine Zn (upper panel) and oxygen preadsorbed Zn system (lower panel). (a) represents the thermodynamically most stable configuration of MeOH adsorption at (10$\bar{1}$0) facet. Methanol adsorption results into substantial reconstruction at the surface. The bare facet of (10$\bar{1}$0) is shown in Fig. SI1-(a). Surface atoms of this facet rearrange themselves and the atomic arrangement resembles to that of (10$\bar{1}$1) facet. (b) depicts the adsorption of MeOH at (10$\bar{1}$1) facet. The extent of reconstruction upon MeOH adsorption is much less compared to (10$\bar{1}$0). (c) Adsorption of MeOH at (10$\bar{1}$3) facet. No reconstruction is observed at this facet upon MeOH adsorption.

Tab.I, the O-H bond does not elongate on the (10$\bar{1}$0) facet of O-Zn because of the adsorption of oxygen below the surface layer resulting into indirect interaction with adsorbed methanol. In the case of (10$\bar{1}$1) and (10$\bar{1}$3), oxygen is present on the surface and hence favors the adsorption of methanol on the surface by forming hydrogen bonds. The strength of the hydrogen bond between O_{surf}-H_{MeOH} determines the activation of methanol on the O-Zn systems. The proximity of surface oxygen and hydrogen of MeOH results in higher activation of the O-H bond of methanol with 9% elongation on the step (10$\bar{1}$3) facet. We computed the activation barrier for dissociation of the O-H bond on all Zn surfaces and oxygen-preadsorbed Zn surfaces. The results are depicted in Fig.2. The energy profile shows that the activation barrier

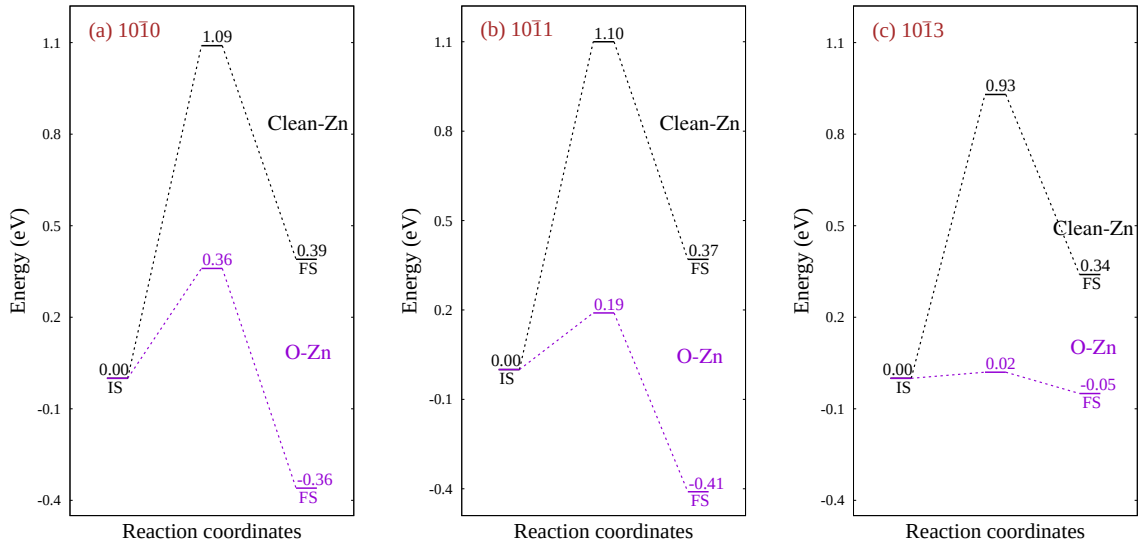

FIG. 2: The activation barrier for O-H bond of MeOH at (a) (10$\bar{1}$0), (b) (10$\bar{1}$1), and (10$\bar{1}$3) facets are shown. In case of flat facets, the activation barrier significantly reduces from clean Zn to O-assisted Zn surface, while for step facet, it becomes negligible. Also, the thermodynamics of reaction become favorable upon oxygen adsorption.

decreases for all three facets upon oxygen adsorption. The barrier for (10$\bar{1}$0) and (10$\bar{1}$1) reduces to one-third and one-fifth respectively, while for the step facet, it becomes almost negligible. Change in reaction energy from positive to negative upon oxygen adsorption makes the reaction exothermic. The presence of oxygen on the surface also helps in stabilizing the hydrogen dissociated from methanol by forming the hydroxide.

The change in the underlying electronic structure upon oxygen adsorption provides a rationale for the observed variation in the reactivity of Zn facets. The 4s levels for Zn metal are close to Fermi and participates in reactivity. Fig.3-(a): (i) and (ii) illustrate the site-specific pDOS of Zn-4s for bare facets of pristine and oxygen-adsorbed surfaces, respectively. The 4s near Fermi, marked in Fig.3-(a), is enlarged and displayed in Fig.3-(b). The magnified plot clearly shows that for the step facet, the intensity of 4s states increases near and at the Fermi level in the oxygen-adsorbed facet compared to the pristine one. In contrast, the 4s intensity decreases near the

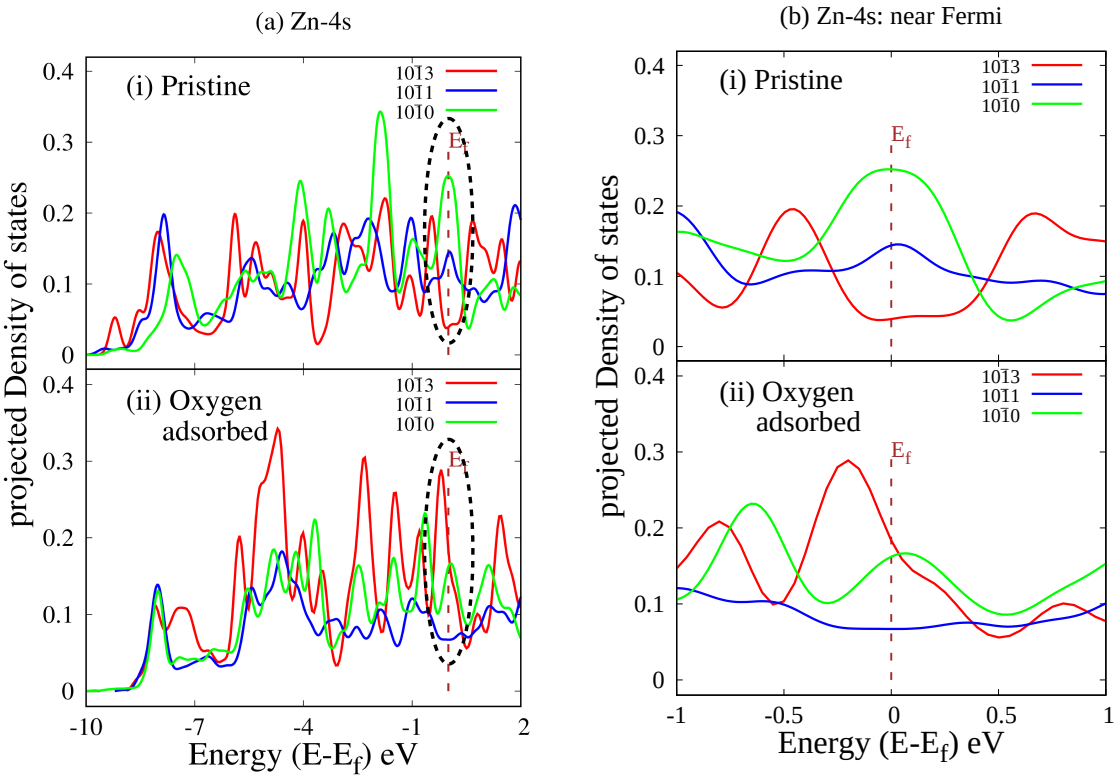

FIG. 3: (a) represents pDOS of 4s levels of pristine Zn surfaces and oxygen adsorbed Zn surfaces. Significant variation in nature of 4s is observed upon oxygen adsorption on Zn surfaces. (b) shows the magnified 4s level near Fermi which are marked in (a). It is clear from the figure that for stepped facets (red curve) the peak intensity increases near Fermi while for both flat facets (blue and green curve) the peak intensity reduces near Fermi as compared to the pristine surfaces.

Fermi level for both the flat facets. The presence of 4s states near the Fermi level facilitates the activation of methanol at the step facet. However, non-zero states at Fermi are not the sole criteria for MeOH activation. Another crucial factor is the presence of surface oxygen in the vicinity of H_{MeOH}. Thus, although the 4s-pDOS are non-zero at Fermi for (10$\bar{1}$0), the absence of surface oxygen near H_{MeOH} results in barely activated MeOH. In the case of (10$\bar{1}$1), although the activation of MeOH is comparable to that of (10$\bar{1}$0), the activation barrier is considerably lower as compared to (10$\bar{1}$0) because of surface oxygen in the vicinity of H_{MeOH}. On the other hand, in

the case of metallic surfaces, the presence of 4s states near Fermi for flat facets do not favour the activation of methanol in the absence of oxygen. Thus, variation in the activity of facets of Zn and O-Zn can be correlated with the electronic structure of the bare facets.

In our previous studies, we discussed the interaction of methanol with several facets of ZnO.[31, 32] We have investigated different flat [$(10\bar{1}0)$, $(10\bar{1}1)$, $(11\bar{2}0)$] and step [$(10\bar{1}3)$, $(11\bar{2}2)$] facets of ZnO for their interaction with methanol. We observed at $(10\bar{1}1)$ facet, methanol spontaneously converts to formaldehyde. These results were validated by experiments and demonstrated that methanol converts to formaldehyde at ZnO nanoparticles at ambient conditions with 100% selectivity. On other flat facets, molecular adsorption is most favorable, while dissociation of MeOH is thermodynamically the most favorable outcome at step facets. The activity of metal oxides can be altered by modifying their structure. ZnO and Al_2O_3 are both used as industrial catalysts for methanol synthesis.[47] In one of the earlier studies by our group, we investigated the interaction of methanol with (220) and (311) facets of $ZnAl_2O_4$.[33] We observed molecular adsorption as well as dissociation of methanol on these facets. Depending upon the site of adsorption, MeOH interacts differently with $ZnAl_2O_4$. We reported that lesser coordinated surface oxygen atoms actively participate in methanol dissociation.

We observe that upon changing the environment of Zn and O in series of different systems (Zn, O-Zn, ZnO, and $ZnAl_2O_4$), the interaction of methanol changes from adsorption to dissociation of O-H as well as C-H bond. To understand this variation, we analyzed different parameters such as interaction energy, Mulliken charges, distance between MeOH and surface metal and/or oxygen atoms for all the facets of all these systems. The interaction energy of the thermodynamically most stable configuration of methanol on various facets of Zn-based systems is noted in Tab.II. The interaction energy for each system is computed by including and excluding the surface reconstruction energy and described as WR and WOR respectively. The numbers in

TABLE II: Interaction energy of methanol on different Zn based systems are reported in the table. Black numbers depict the energy of metallic Zn and O-Zn systems. Blue and red colored numbers represent interaction of methanol at ZnO, and $ZnAl_2O_4$ facets respectively. Adsorption of methanol on these different system triggers surface reconstruction which reflects in the interaction energy. WR (with reconstruction) stands for energy with the impact of reconstruction. However, in order to homogenize the energies, we have eliminated the reconstruction effect from interaction as demonstrated by WOR (without reconstruction).

systems/facets		$(10\bar{1}0)$/220	$(10\bar{1}1)$/311	$(10\bar{1}3)$	$(11\bar{2}0)$	$(11\bar{2}2)$
Zn	WR	-4.09	-1.36	-0.66		
	WOR	-0.77	-0.69	-0.68		
O-Zn	WR	-3.26	-0.72	-1.01		
	WOR	-0.78	-0.60	-1.13		
ZnO	WR	-1.58	**-7.95**	**-3.88**	-1.24	**-6.24**
	WOR	-1.90	**-4.83**	**-2.91**	-1.40	**-3.38**
$ZnAl_2O_4$	WR	**-1.81**	**-4.14**			
	WOR	**-2.47**	**-4.91**			

black represent interaction energy of methanol with Zn and O-Zn surfaces, while blue and red numbers indicate ZnO and $ZnAl_2O_4$ surfaces respectively. The numbers in bold signify dissociation of methanol as thermodynamically most stable outcome on that facet. It is clear from the interaction energies (computed for both the WR and WOR) of Tab.II that the presence of oxygen facilitates the adsorption of MeOH on step facet of O-Zn. We do not observe any correlation between the interaction energy (WR) and outcome of the interaction. However, the extent of reconstruction varies from facet to facet. And hence, upon normalization of the energies by excluding the impact of reconstruction (WOR), there is a one-to-one correlation between interaction energies (WOR) and outcome of MeOH. Dissociation is always associated with lower interaction energy than the molecular adsorption. Also, irrespective of the outcome, methanol interaction is more favored on the ZnO and $ZnAl_2O_4$ facets as compared to

Zn and O-Zn.

TABLE III: Mulliken charges on surface zinc atoms of Zn, O-Zn, ZnO, and $ZnAl_2O_4$. For Zn, and O-Zn the charges are shown in black color, whereas for ZnO and $ZnAl_2O_4$, the charges are represented in blue and red color respectively. Charges for the facets where dissociation of MeOH occurs, are shown in bold numbers. Transfer of electron from metal to oxygen is evident from the effective charges on Zn.

systems/facets	$(10\bar{1}0)$/220	$(10\bar{1}1)$/311	$(10\bar{1}3)$	$(11\bar{2}0)$	$(11\bar{2}2)$
Zn	0.05	0.12	0.19(0.14)		
O-Zn	0.49	0.61	0.50		
ZnO	**0.85**	**1.04**	0.96(**0.64**)	0.96	**0.81**
$ZnAl_2O_4$	**1.52**	**1.53**(1.58)			

TABLE IV: Mulliken charges on surface oxygen atoms of O-Zn(black color), ZnO(blue color), and $ZnAl_2O_4$(red color). The shortest distance between oxygen and surface atom (BL) is also shown

systems/facets	property	$(10\bar{1}0)$/220	$(10\bar{1}1)$/311	$(10\bar{1}3)$	$(11\bar{2}0)$	$(11\bar{2}2)$
O-Zn	charge(e)	-0.74	-0.81	-1.38		
	BL(Å)	1.93	1.89	1.88		
ZnO	charge(e)	**-0.79**	**-0.68**	**-0.82**(-0.89)	-0.89	**-0.85**
	BL(Å)	1.77	1.85	1.94(1.87)	1.90	1.82
$ZnAl_2O_4$	charge(e)	**-1.03**(-1.07)	**-1.00**(-1.11; -1.17)			
	BL(Å)	1.82(1.74)	1.77(1.93; 1.85)			

Next, we note effective charges on surface zinc and oxygen atoms for all the facets investigated in Tab.III and Tab.IV, respectively. The numbers in black depict Zn and O-Zn systems, whereas the blue and red numbers indicate ZnO and $ZnAl_2O_4$ systems. It is clear from Tab.III that with increasing oxygen content Zn becomes more positive, indicating electron transfer from metal to oxygen. Similarly, as seen

from Tab.IV, charge gained by oxygen atoms varies from -0.68 for ZnO($10\bar{1}1$) to -1.38 for O-Zn($10\bar{1}3$). However, we do not see any correlation between the charge on surface zinc/oxygen and the outcome of the interaction i.e. adsorption or dissociation of MeOH.

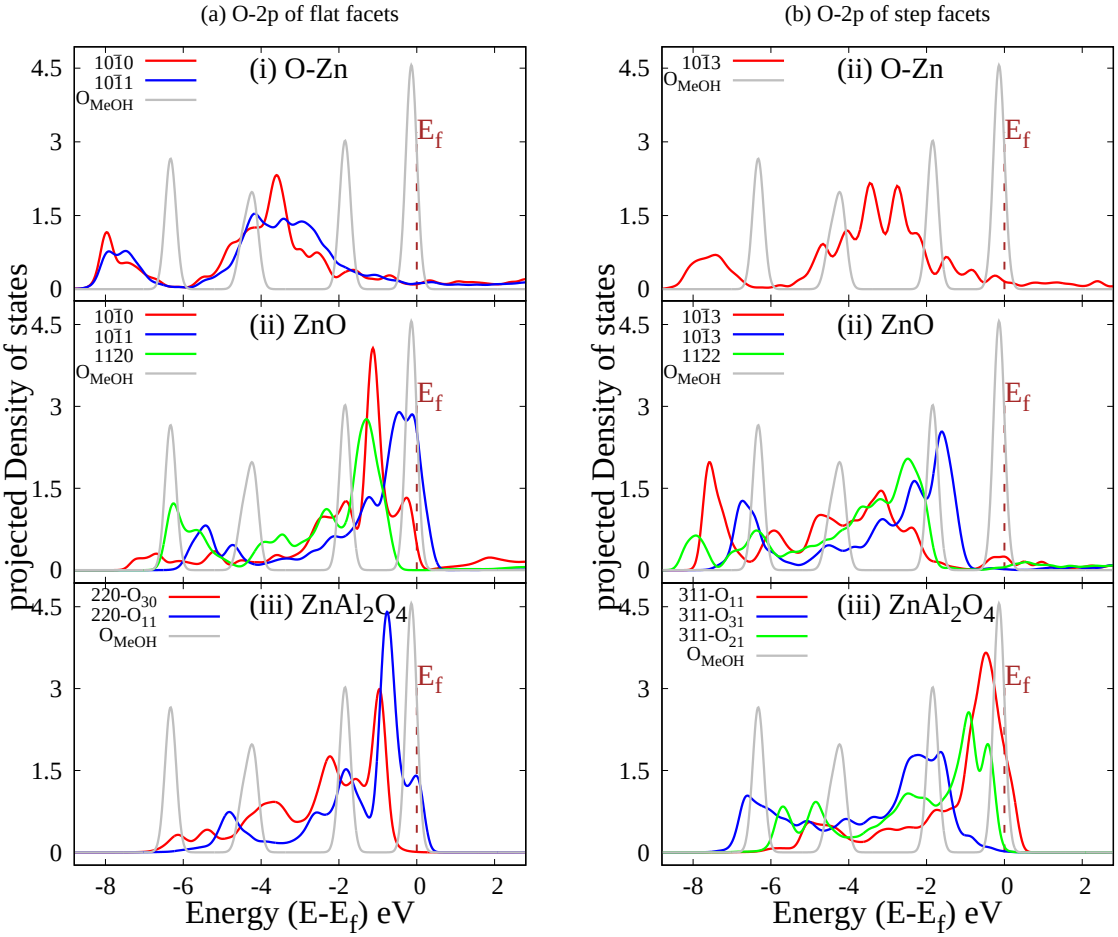

FIG. 4: pDOS of $2p$ of O in different systems (i) oxygen preadsorbed zinc (O-Zn), (ii) metal oxide (ZnO), (iii) mixed metal oxide ($ZnAl_2O_4$). (a) shows flat facets while (b) represents stepped facets. $2p$ of oxygen of methanol is plotted in gray color for reference.

Next, we compare pDOS for O-$2p$ of O-Zn, ZnO, and $ZnAl_2O_4$ for flat and step facets as shown in Fig.4-(a) and (b), respectively. The reference pDOS for $2p$ of O_{MeOH} is plotted in each figure as a gray curve. Depending on the environment

the pDOS exhibit subtle variation which influences the outcome of the interaction of MeOH with that facet. Two flat facets [$(10\bar{1}0)$ and $(10\bar{1}1)$] and step facets of ZnO with non zero pDOS at Fermi favours dissociation of MeOH. Whereas for $(11\bar{2}0)$ facet, there are no states at Fermi level and this is the facet of ZnO with chemisorption of MeOH as the only outcome. For both step facets of ZnO (see (ii) of Fig.4-(b)) significantly low number of O-2p states are present near Fermi. However, for both these stepped facets, Zn-4s states are present at Fermi (shown in Fig. SI-3-(b)-(iii)) and overlaps with 2p states of O_{MeOH}, which accounts for the spontaneous dissociation of MeOH on these facets. This site specific signature of pDOS is also observed in the tDOS plot which reflects the underlying electronic structure of the entire facet. The tDOS plots of flat and step facets of all systems are shown in Fig.5-(a) and (b) respectively. The next system we will discuss is a mixed metal oxide, $ZnAl_2O_4$. For $ZnAl_2O_4$, on (220) and (311) facets dissociation of MeOH is the favoured outcome. Al acts as the active site for methanol adsorption in these cases because of its greater affinity for oxygen than Zn. Surface oxygen atoms have variations in their coordination with Zn and Al atoms. The difference in the coordination of these oxygen atoms also reflects in their pDOS plots as seen in Fig.4-(a) and (b)-iii. These different 'types' of oxygen atoms on the surface are denoted based on their coordination with Al and Zn atoms, respectively. For example, the key 220-O_{30} in Fig.4-a-(iii) represents the pDOS of the oxygen atom, which is coordinated with 3 Al atoms. Interestingly, when MeOH is placed near the oxygen atoms having non-zero states at the Fermi, they undergo dissociation. In contrast, if MeOH is placed near oxygen atoms which do not have states at Fermi, then they are chemisorbed. Thus, the adsorption of MeOH in the vicinity of oxygen, which has non-zero energy states at Fermi, is essential for dissociating methanol. However, it is not sufficient to have non-zero states at Fermi. The orientation of methanol plays a crucial role in determining the outcome. The preferred orientation is where H_{MeOH} is inclined towards the O_{surf}. Fig.6 represents two different orientations of methanol on (220) facet of $ZnAl_2O_4$. The atoms displayed in blue depict those oxygen atoms

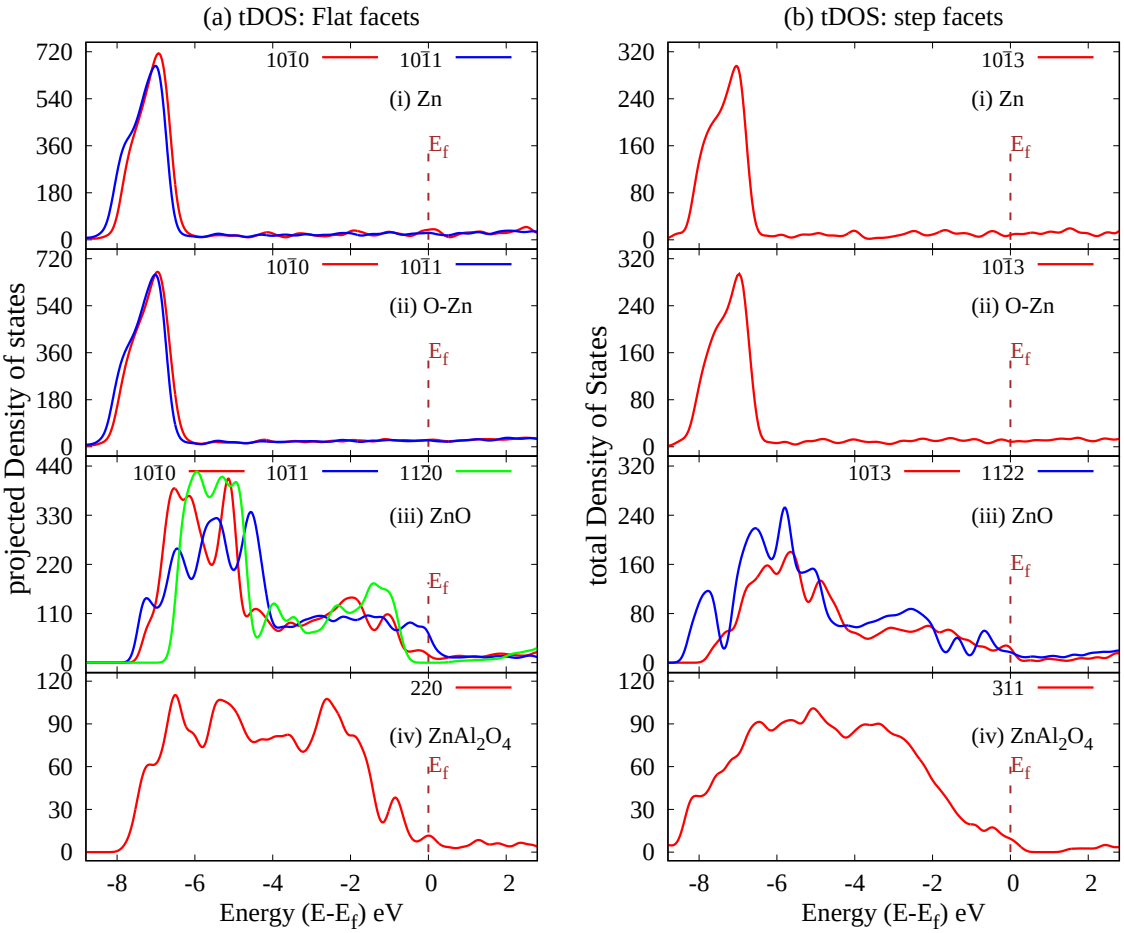

FIG. 5: tDOS of different systems (i) metallic Zn, (ii) oxygen preadsorbed zinc (O-Zn), (iii) metal oxide (ZnO), (iv) mixed metal oxide ($ZnAl_2O_4$). (a) shows flat facets while (b) represents stepped facets.

with non-zero peaks at the Fermi level, and the red ones have zero energy states at the Fermi level. Fig.6-(a) and (b) show the adsorption of methanol on the same Al atom in two different orientations, which results in adsorption and dissociation of methanol, respectively. The favoured orientation of methanol (refer Fig.6-(b)) for dissociation is the one in which H_{MeOH} is tilted towards the blue-coloured oxygen atom, which has non-zero energy states at Fermi. This observation holds for the (311) facet also. It is interesting to note that this trend is also visible in the pDOS plot of each facet, where Al-3p is present at Fermi (Fig. SI-4) and overlaps with 2p of O_{MeOH}, but no

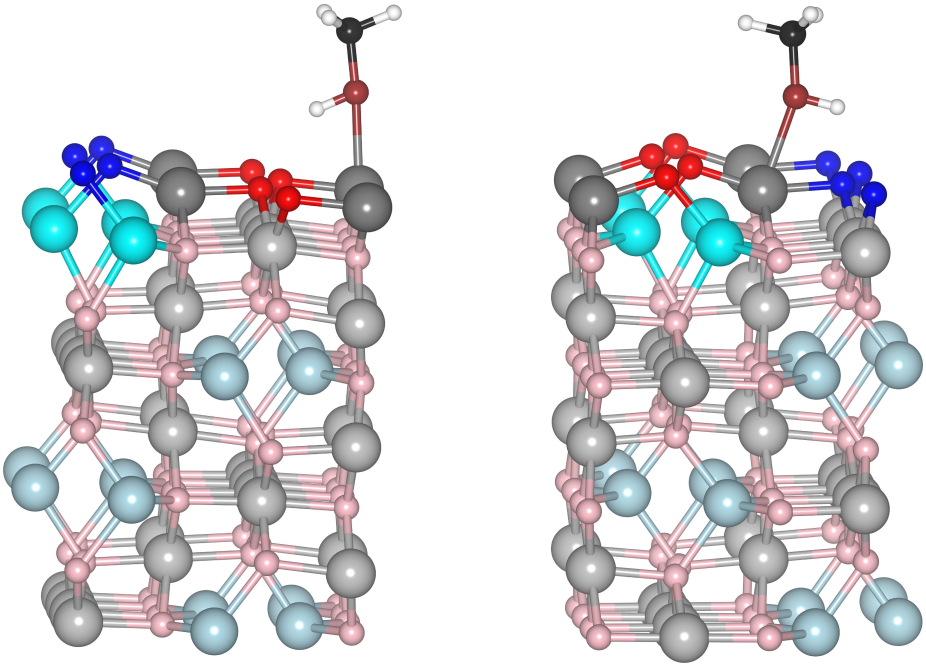

FIG. 6: The orientation of methanol on (220) facet of $ZnAl_2O_4$ are shown. The atoms in blue color corresponds to those oxygens which have non-zero energy states at Fermi as shown in Fig.4-(a)-(iii) and red are those which have zero energy states at Fermi. (a) shows the initial position of methanol where the H_{MeOH} is inclined towards red oxygen atoms and results into adsorption of methanol upon optimization. (b) depicts the initial position of methanol in which H_{MeOH} is tilted towards blue oxygen atoms result into dissociation. This signifies that along with presence of oxygen with non-zero peak at Fermi, orientation of MeOH does play a crucial role in determining the outcome of interaction of MeOH in complex system such as $ZnAl_2O_4$.

Zn-4s is seen around Fermi (Fig. SI-3). This signature is also clearly seen in the tDOS of $ZnAl_2O_4$ depicted in Fig.5-(iv).

IV. CONCLUSION

To conclude, we have demonstrated a one-to-one correlation between the availability of DOS at the Fermi and the dissociation of MeOH by investigating the interaction of MeOH with various Zn-based catalysts. To our knowledge, no studies have been reported on the interaction of methanol with zinc surfaces. The current study

thoroughly examines how methanol interacts with zinc and oxygen-preadsorbed zinc surfaces. Since the most prominent facets in the XRD of bulk Zn are $(10\overline{1}0)$, $(10\overline{1}1)$, and $(10\overline{1}3)$, we investigated these facets for interaction with methanol. Physisorption of MeOH is a common outcome on all the facets of pristine Zn with a substantial reconstruction of $(10\overline{1}0)$ surface. We observed the chemisorption of MeOH on the step facet of oxygen-preadsorbed Zn and physisorption on pristine Zn. Thus, oxygen adsorption enhances the reactivity of the surface with methanol. Oxygen adsorption significantly lowers the activation barrier for O-H bond dissociation, with a negligible barrier on the step facet. The dissociation of the O-H bond also changes from being endothermic on pristine Zn surfaces to exothermic on oxygen-preadsorbed surfaces. Finally, we discuss the underlying electronic structures of different catalytic systems, including Zn, O-Zn, ZnO, and $ZnAl_2O_4$, that have been investigated for interactions with methanol in our current and earlier studies. By carefully analyzing the site-specific pDOS plots of these facets, we report that the existence of energy states of oxygen, metal, or both at or near the Fermi level has a substantial influence on the dissociation of MeOH on that particular facet. With this knowledge, we may examine catalytic surfaces for their interactions with incoming adsorbate species from a fresh perspective.

V. ACKNOWLEDGEMENT

CSIR-4PI is gratefully acknowledged for the computational facility.

---

[1] S.A Sardar, J.A Syed, K Tanaka, F.P Netzer, and M.G Ramsey. The aluminium-alcohol interface: Methanol on clean Al(111) surface. *Surface Science*, 519(3):218–228, 2002.

[2] Marilena Carbone and Karin Larsson. Methanol adsorption on the Si(100)-2x1 surface: a first-principles calculation. *Journal of Physics: Condensed Matter*, 17(8):1289–1300, feb 2005.

[3] Do Hwan Kim, Sung-Soo Bae, Suklyun Hong, and Sehun Kim. Atomic and electronic structure of methanol on Ge(100). *Surface Science*, 604(2):129–135, 2010.

[4] Susumu Yanagisawa, Takao Tsuneda, Kimihiko Hirao, and Yoichi Matsuzaki. Theoretical investigation of adsorption of organic molecules onto Fe (110) surface. *Journal of Molecular Structure: THEOCHEM*, 716(1-3):45–60, 2005.

[5] Ana S. Moura, Jose L. C. Fajín, Ana S. S. Pinto, Marcos Mandado, and M. Natália D. S. Cordeiro. Competitive paths for methanol decomposition on ruthenium: A DFT study. *The Journal of Physical Chemistry C*, 119(49):27382–27391, 2015.

[6] Xinzheng Yang. Mechanistic insights into ruthenium-catalyzed production of H_2 and CO_2 from methanol and water: A DFT study. *ACS Catalysis*, 4(4):1129–1133, 2014.

[7] Zeb C. Kramer, Xiang-Kui Gu, Dingyu D. Y. Zhou, Wei-Xue Li, and Rex T. Skodje. Following molecules through reactive networks: Surface catalyzed decomposition of methanol on Pd(111), Pt(111), and Ni(111). *The Journal of Physical Chemistry C*, 118(23):12364–12383, 2014.

[8] Ruibin Jiang, Wenyue Guo, Ming Li, Dianling Fu, and Honghong Shan. Density functional investigation of methanol dehydrogenation on Pd(111). *The Journal of Physical Chemistry C*, 113(10):4188–4197, 2009.

[9] Ya-Hui Fang and Zhi-Pan Liu. First principles tafel kinetics of methanol oxidation on Pt(111). *Surface Science*, 631:42–47, 2015.

[10] Xiang-Kui Gu and Wei-Xue Li. First-principles study on the origin of the different selectivities for methanol steam reforming on Cu(111) and Pd(111). *The Journal of Physical Chemistry C*, 114(49):21539–21547, 2010.

[11] Alejandro Montoya and Brian S. Haynes. Methanol and methoxide decomposition on silver. *The Journal of Physical Chemistry C*, 111(27):9867–9876, 2007.

[12] Lei Wang, Chaozheng He, Wenhua Zhang, Zhenyu Li, and Jinlong Yang. Methanol-selective oxidation pathways on Au surfaces: A first-principles study. *The Journal of Physical Chemistry C*, 118(31):17511–17520, 2014.

[13] Sung Sakong and Axel Gross. Total oxidation of methanol on Cu(110): a density functional theory study. *The Journal of Physical Chemistry A*, 111(36):8814–8822, 2007.

[14] Donghai Mei, Lijun Xu, and Graeme Henkelman. Potential energy surface of methanol decomposition on Cu(110). *The Journal of Physical Chemistry C*, 113(11):4522–4537, 2009.

[15] Roey Ben David, Adva Ben Yaacov, Ashley R. Head, and Baran Eren. Methanol decomposition on copper surfaces under ambient conditions: Mechanism, surface kinetics, and structure sensitivity. *ACS Catalysis*, 12(13):7709–7718, 0.

[16] Ye Xu, Jeff Greeley, and Manos Mavrikakis. Effect of subsurface oxygen on the reactivity of the Ag(111) surface. *Journal of the American Chemical Society*, 127(37):12823–12827, 2005.

[17] Gui-Chang Wang, Shu-Xia Tao, and Xian-He Bu. A systematic theoretical study of water dissociation on clean and oxygen-preadsorbed transition metals. *Journal of Catalysis*, 244(1):10–16, 2006.

[18] Jooho Kim, Enrique Samano, and Bruce E. Koel. CO adsorption and reaction on clean and oxygen-covered Au(211) surfaces. *The Journal of Physical Chemistry B*, 110(35):17512–17517, 2006.

[19] Shiyi Wang, Enbo Zhu, Yu Huang, and Hendrik Heinz. Direct correlation of oxygen adsorption on platinum-electrolyte interfaces with the activity in the oxygen reduction reaction. *Science Advances*, 7(24):eabb1435, 2021.

[20] Ping Liu and Jens Kehlet Nørskov. Ligand and ensemble effects in adsorption on alloy surfaces. *Physical Chemistry Chemical Physics*, 3(17):3814–3818, 2001.

[21] Shu-Xia Tao, Gui-Chang Wang, and Xian-He Bu. Effect of pre-covered oxygen on the dehydrogenation reactions over copper surface: a density functional theory study. *The Journal of Physical Chemistry B*, 110(51):26045–26054, 2006.

[22] M. Natália D.S. Cordeiro, Ana S.S. Pinto, and José A.N.F. Gomes. A DFT study of the chemisorption of methoxy on clean and low oxygen precovered Ru(0001) surfaces. *Surface Science*, 601(12):2473–2485, 2007.

[23] Bingjun Xu, Jan Haubrich, Thomas A Baker, Efthimios Kaxiras, and Cynthia M Friend. Theoretical study of o-assisted selective coupling of methanol on Au (111). *The Journal of Physical Chemistry C*, 115(9):3703–3708, 2011.

[24] Hassan Aljama, Jong Suk Yoo, Jens K. Nørskov, Frank Abild-Pedersen, and Felix Studt. Methanol partial oxidation on Ag(111) from first principles. *ChemCatChem*, 8(23):3621–3625, 2016.

[25] Shahin Goodarznia and Kevin J. Smith. Properties of alkali-promoted Cu-MgO catalysts and their activity for methanol decomposition and C2-oxygenate formation. *Journal of Molecular Catalysis A: Chemical*, 320(1):1–13, 2010.

[26] Øyvind Borck and Elsebeth Schröder. First-principles study of the adsorption of methanol at the α-Al_2O_3 (0001) surface. *Journal of Physics: Condensed Matter*, 18(1):1, 2005.

[27] Mariia Merko, G. Wilma Busser, and Martin Muhler. Non-oxidative dehydrogenation of methanol to formaldehyde over bulk β-Ga_2O_3. *ChemCatChem*, 14(13):e202200258, 2022.

[28] Feg-Wen Chang, Hsin-Yin Yu, L Selva Roselin, and Hsien-Chang Yang. Production of hydrogen via partial oxidation of methanol over Au/TiO_2 catalysts. *Applied catalysis A: general*, 290(1-2):138–147, 2005.

[29] Zhao Liu, Charles C Sorrell, Pramod Koshy, and Judy N Hart. Dft study of methanol adsorption on defect-free CeO_2 low-index surfaces. *ChemPhysChem*, 20(16):2074–2081, 2019.

[30] Navid Abedi, Philipp Herrmann, and Georg Heimel. Methanol on ZnO ($10\overline{1}0$): From adsorption over initial dehydrogenation to monolayer formation. *The Journal of Physical Chemistry C*, 119(37):21574–21584, 2015.

[31] Shweta Mehta and Kavita Joshi. From molecular adsorption to decomposition of methanol on various ZnO facets: A periodic DFT study. *Applied Surface Science*, 602:154150, 2022.

[32] Shweta Mehta, Mirabai Kasabe, Shubhangi Umbarkar, and Kavita Joshi. Methanol to formaldehyde at ambient condition: from computation to experiments. *to be communicated*, 2022.

[33] Shweta Mehta, Sheena Agarwal, Nivedita Kenge, Siva Prasad Mekala, Vipul Patil, T Raja, and Kavita Joshi. Mixed metal oxide: A new class of catalyst for methanol activation. *Applied Surface Science*, 534:147449, 2020.

[34] P. E. Blöchl. Projector augmented-wave method. *Physical Review B*, 50(24):17953–17979, 1994.

G. Kresse and D. Joubert. From ultrasoft pseudopotentials to the projector augmented-wave method. *Physical Review B*, 59(3):1758–1775, 1999.

[35] John P. Perdew, Kieron Burke, and Matthias Ernzerhof. Generalized gradient approximation made simple [phys. rev. lett. 77, 3865 (1996)]. *Physical Review Letters*, 78(7):1396–1396, 1997.

[36] G. Kresse and J. Hafner. *Ab initio* molecular-dynamics simulation of the liquid-metal–amorphous-semiconductor transition in germanium. *Physical Review B*, 49(20):14251–14269, 1994.

G. Kresse and J. Furthmüller. Efficient iterative schemes for *ab initio* total-energy calculations using a plane-wave basis set. *Physical Review B*, 54(16):11169–11186, 1996.

G. Kresse and J. Furthmüller. Efficiency of ab-initio total energy calculations for metals and semiconductors using a plane-wave basis set. *Computational Material Science*,

6(1):15–50, 1996.

[37] Anubhav Jain, Shyue Ping Ong, Geoffroy Hautier, Wei Chen, William Davidson Richards, Stephen Dacek, Shreyas Cholia, Dan Gunter, David Skinner, Gerbrand Ceder, et al. Commentary: The materials project: A materials genome approach to accelerating materials innovation. *Applied Materials*, 1(1):011002, 2013.

[38] Kei Iokibe, Kazuhisa Azumi, and Hiroto Tachikawa. Surface diffusion of a Zn adatom on a Zn(001) surface: a DFT study. *The Journal of Physical Chemistry C*, 111(36):13510–13516, 2007.

[39] Daniele Stradi, Line Jelver, Søren Smidstrup, and Kurt Stokbro. Method for determining optimal supercell representation of interfaces. *Journal of Physics: Condensed Matter*, 29(18):185901, 2017.

[40] Stefan Grimme. Semiempirical GGA-type density functional constructed with a long-range dispersion correction. *Journal of computational chemistry*, 27(15):1787–1799, 2006.

[41] Richard Dronskowski and Peter E Blöchl. Crystal orbital hamilton populations (COHP): energy-resolved visualization of chemical bonding in solids based on density-functional calculations. *The Journal of Physical Chemistry*, 97(33):8617–8624, 1993.

Volker L Deringer, Andrei L Tchougréeff, and Richard Dronskowski. Crystal orbital hamilton population (COHP) analysis as projected from plane-wave basis sets. *The Journal of Physical Chemistry A*, 115(21):5461–5466, 2011.

Stefan Maintz, Volker L Deringer, Andrei L Tchougréeff, and Richard Dronskowski. Analytic projection from plane-wave and PAW wavefunctions and application to chemical-bonding analysis in solids. *Journal of Computational Chemistry*, 34(29):2557–2567, 2013.

Stefan Maintz, Volker L Deringer, Andrei L Tchougréeff, and Richard Dronskowski. Lobster: A tool to extract chemical bonding from plane-wave based DFT. *Journal of Computational Chemistry*, 37(11):1030–1035, 2016.

[42] Graeme Henkelman, Blas P. Uberuaga, and Hannes Jónsson. A climbing image nudged elastic band method for finding saddle points and minimum energy paths. *The Journal of Chemical Physics*, 113(22):9901–9904, 2000.

[43] Silvia Mostoni, Paola Milana, Barbara Di Credico, Massimiliano D'Arienzo, and Roberto Scotti. Zinc-based curing activators: New trends for reducing zinc content in rubber vulcanization process. *Catalysts*, 9(8), 2019.

[44] Salahudeen Shamna, C. M. A. Afsina, Rose Mary Philip, and Gopinathan Anilkumar. Recent advances and prospects in the Zn-catalysed mannich reaction. *RSC Adv.*, 11:9098–9111, 2021.

[45] Wesley Sattler and Gerard Parkin. Zinc catalysts for on-demand hydrogen generation and carbon dioxide functionalization. *Journal of the American Chemical Society*, 134(42):17462–17465, 2012. PMID: 23046174.

[46] MS Spencer. The role of zinc oxide in Cu/ZnO catalysts for methanol synthesis and the water–gas shift reaction. *Topics in Catalysis*, 8(3):259–266, 1999.

[47] Malte Behrens, Felix Studt, Igor Kasatkin, Stefanie Kühl, Michael Hävecker, Frank Abild-Pedersen, Stefan Zander, Frank Girgsdies, Patrick Kurr, Benjamin-Louis Kniep, et al. The active site of methanol synthesis over $Cu/ZnO/Al_2O_3$ industrial catalysts. *Science*, 336(6083):893–897, 2012.